VOL. 12, NO. 24, DECEMBER 2017 ISSN 1819-6608
ARPN Journal of Engineering and Applied Sciences

www.arpnjournals.com

COMPACT QUAD-BAND BPF DESIGN WITH FRACTAL STEPPED-IMPEDANCE RING RESONATOR

Hadi T. Ziboon and Jawad K. Ali
Microwave Research Group, Department of Electrical Engineering, University of Technology, Iraq
E-Mail: jawadkali@theiet.org

ABSTRACT

This paper presents the design of new miniaturized multiband microstrip bandpass filters (BPFs) for multi-services wireless applications. The introduced filter structures are the results of the implementation of the fractal-based topology together with the stepped impedance resonator (SIR) technique on the conventional square loop resonator. Three microstrip BPFs have been investigated corresponding to the first three Minkowski fractal iterations as applied to the SIR ring resonator. The first bandpass filter, which corresponds to the zero fractal iteration, has been designed at 5.8 GHz for wireless local area network (WLAN) applications. The proposed filter has been etched using a substrate with an insulation constant of 10.8, a thickness of 1.27 mm and loss tangent of 0.0023. Based on this filter, the other two filters have been designed by applying the Minkowski fractal geometries of the 1st and 2nd iterations. Results reveal that the three filters offer size reduction percentages of about 40%, 56%, and 63% as compared with the conventional dual-mode square ring resonator. The simulated and experimental results of the first BPF prototype are well-matched.

Keywords: compact bandpass filter, fractal-based BPF, multiband BPF, stepped-impedance ring resonator, fractal geometry.

1. INTRODUCTION

Bandpass filters, designed at microwave and RF play a significant role in communication systems. Because of the large number of radar, satellite, and mobile wireless systems, there is a continuing demand for design techniques that can satisfy the ever-increasing requirements for accuracy, reliability, and improved performance [1]. On the other hand, the compact size of the modern communication system makes the designers encounter new challenges that the designed filters have to be small and slim. For that, the microstrip planar filters are found to be a better choice compared to the waveguide filters for instance. Another challenge the designers have to come across is that the filters are being with multiband resonant characteristic to fulfill the requirements of multi-services wireless applications. However, high-quality filters are characterized by other specifications, beside the small size. High-quality filters should have a high out of the band rejection and passbands with good skirt response and a roll-off rate at both edges of the passband.

Filter miniaturization can be carried out using many methods with various degrees of performance improvement levels. Using high substrates with high dielectric constants will add additional losses; making this choice less attractive [2]. Another option to design compact size bandpass filters is to make use of the dual-mode resonators in the filter implementation. In this case, the size of the resulting filter is only half of that using the single-mode resonator [3]. Dual-mode behavior is the simultaneous propagation of two modes whose resonant frequencies are not harmonically related. Strictly speaking, dual-mode resonators are only those resonators that support two modes that resonate at similar frequencies, but each has its distinct field distribution. Dual-mode resonators with perturbation were first applied in single-band filters. A resonator with coupled resonances acts as a structure with two coupled resonators, i.e., as a filter of the second order. Thus, by mode coupling, a structure with two transmission poles is achieved which provides an excellent performance of the filter regarding the insertion loss and the quality factor. It is clear that using this method; the size reduction will be more practical when designing higher order bandpass filters. In single-band filters, the resonators used are usually dual-mode, which reduces the number of resonators needed for the realization of the specified filter function [4]. An illustrative example of a single-band filter built using a dual-mode resonator with perturbation is presented in [5]. One meander-shaped ring resonator with perturbation comprises the filter that exhibits a passband with two transmission poles, which implies dual-mode behavior of the resonator. Additional size reduction might be obtained when implementing fractal geometries to the dual-mode resonators [6]. Employing Minkowski fractal variant to the square dual-mode microstrip resonator results in considerable size reduction of the dimensions of the filter presented in [6].

On the other hand, stepped-impedance multi-mode resonators (SIR) are chosen in designing of multiband filters [7-10]. There is a considerable potential of SIR for high-performance dual-band filter design. Furthermore, multi-band BPFs have been developed using stub-loaded resonators (SLR). These filter configurations provide dual-mode and tri-mode resonant behavior. Such resonators were first introduced to design BPFs in [11]. Many SLR based BPF structures with comparable performance have been presented in [11-15]. These structures consist of ring-shaped SLRs, but they adopt different schemes to provide transmission zeros. The filter structures in [12] and [13] use asymmetric feeding, while the filter in [14] employs in an inductive cross-coupling and the structure in [15] uses source load coupling.

Furthermore, multi-band BPFs have been designed using stub-loaded SIRs [16-18]. This configuration is composed of a SIR loaded by one or more open stubs. The filter structure reported in [16] consists of an S-shaped stepped-impedance resonator loaded by the two same open stubs to tune the second resonant band to a certain extent. The filter structure reported in [17] is composed of inductively fed hairpin stepped-impedance resonators that are loaded with stubs in the midpoint. The BPF structure proposed in [18] consists of a grounded SIR loaded with folded stubs that are symmetrically and centrally attached on the resonator.

Recently, dual-mode resonators are employed in the design of multiband BPFs. The dual-mode behavior of resonators with perturbation can be used in several manners to obtain dual-band response. The first way is to use two coupled degenerative modes as sources of two separate passbands. This has been applied only in a few configurations since the positioning of two degenerative modes on relatively distant frequencies requires a robust coupling between the modes which makes the filter design more complex. The configuration presented in [5] employs a dual-mode square patch resonator with a perturbation with the shape of a cross. By varying different geometrical parameters of the cross slot, the resonant frequency of one mode can be changed independently of the resonant frequency of the other mode. Also, the configuration of the feeding lines allows transmission zeros to occur. Although this filter is a very smart dual-band solution, which enables independent control of one passband, it is also characterized by poor selectivity in the second passband as well as by relatively large overall dimensions.

To gain more size reduction of the filter design, fractal geometries are found to an excellent choice. Two unique features designate different fractal geometries. These features are the space-filling and the self-similarity. Fractal properties have opened new and basic methods for antennas and electronic solutions in the course of the most recent 25 years. Additionally, fractals give another era of optimized design tools, initially utilized effectively in antennas but applicable in a general manner [19]. As a consequence, the shape of planar resonators is based on the fractal iterations. It is recognized that the application of fractal iterations to shape the resonator is repeatable and follows a systematic method. It is shown that for a given resonant frequency, a resonator based on fractal iterations can become significantly smaller than conventional planar resonators. It is also shown that by increasing the number of fractal iterations, the resonators can be reduced further. Furthermore, fractal geometries have been applied to the conventional microstrip resonators which are successfully adopted to design compact microwave microstrip filters and planar circuits. Based on the conventional square patch, Sierpinski carpet has been applied to design a dual-mode microstrip bandpass filter [20-21].

Other fractal geometries, such as Hilbert, Moore, and Koch have also been adopted to design miniaturized bandpass filters [22-27]. Peano fractal geometries have been successfully applied to the conventional resonators to produce high performance miniaturized single mode and dual-mode microstrip bandpass filters [28-30]. The large space-filling property of this fractal geometry makes it an attractive choice to design bandpass filters with high size reduction levels. Minkowski fractal based microstrip resonators have more attracted microwave filter designers to be successfully applied to produce compact dual-mode microstrip ring resonator BPFs, owing to its high space-filling property [31-39].

The microstrip BPF suggested in this paper is based on a new design methodology to get more size reduction together with the multiband response using a single resonator. This resonator has been modeled in two steps; in the first step, the SIR approach has been used on all sides of the closed square loop resonator. In the second step, modified variant of the 1st and 2nd iteration Minkowski fractal curves have been applied to produce the proposed microstrip dual-mode SIR BPFs. Besides the miniaturized size, the resulting BPFs have been shown to offer reasonable dual-band and multiband responses with high insertion loss in the out of the passbands. The resulting BPF offers a compact size which makes it easily integrated with most of the recently available compact wireless devices. The performance of this filter has been demonstrated by experimental measurements.

2. THE STEPPED IMPEDANCE RESONATOR

The dual-mode behavior can also be achieved in the structures that do not support degenerative modes. In that case, the two modes do not stem from coupled degenerative modes, but they are formed by the fundamental and higher-order mode whose resonant frequencies are not harmonically related as in conventional structures. In other words, the dual-mode behavior occurs in configurations that do not represent classical dual-mode resonators, but they have perturbations that cause a change in the ratio of resonant frequencies. An example of such configuration is the stepped-impedance resonator (SIR), Figure-2. 20, which was proposed for the first time in [40]. It can be said that the SIR originates from the conventional microstrip resonator, in which a stepped-impedance perturbation is introduced. The SIR approach has the facility of being easy to be built and the extra size reduction it offers. However, its performance degrades and becomes unsuitable for frequencies above 20 GHz because of the radiations, transverse resonances. Figure-1 shows the configuration of the primary stepped-impedance resonator structure and the equivalent circuits of the even and odd modes.

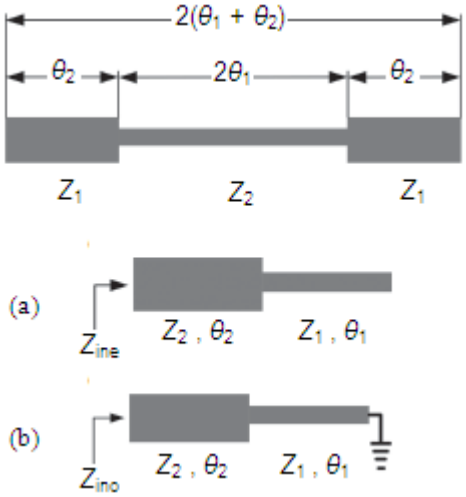

Figure-1. The configuration of stepped-impedance resonator; (a) even mode, and (b) odd mode [5].

Due to its symmetry, SIR can be analyzed using even-/odd-mode analysis. The even and odd equivalent circuits are shown in Figure-1, and the expressions for the even and odd input impedances are the following:

$$Z_{ine} = jZ_2 \frac{Z_2 \tan\theta_1 \tan\theta_2 - Z_1}{Z_1 \tan\theta_2 + Z_2 \tan\theta_1} \quad (1)$$

$$Z_{ino} = jZ_2 \frac{Z_1 \tan\theta_1 + Z_2 \tan\theta_2}{Z_2 - Z_1 \tan\theta_1 \tan\theta_2} \quad (2)$$

where Z_1 and Z_2 are the characteristic impedances, θ_1 and θ_2 their electrical lengths, and K the ratio of Z_2/Z_1. From the resonant condition $1/Z_{in} = 0$, the fundamental resonance can be determined as [5]:

$$K = \tan\theta_1 \tan\theta_2 \quad (3)$$

3. THE MINKOWSKI FRACTAL GEOMETRY

The length segments x or y or both of the SIR resonator, shown in Figure-1, might be made with a fractal shape to get miniaturization besides the multimode response. In this work, a modified variant of the Minkowski fractal geometry, of the 1st and 2nd iterations, has been supposed to perform such a task. Figure-2 exhibits the generation process of the Minkowski-like fractal geometry used to shape a square shape ring. As will be shown in the following sub-sections, dual-mode SIR resonators based on the modified Minkowski fractal geometry are adopted to design compact BPFs with multiband responses for use in a wide variety of wireless communication applications.

Figure-2. The steps of growth of the modified Minkowski fractal structure: (a) the generator, (b) the square ring, (c) the 1st iteration, and (d) the 2nd iteration [6].

It has been confirmed that shape change of the structure described in Figures 2(c) and 2(d) are means to enhance the surface current path length associated with that of the traditional square ring resonator. Consequently, a reduced resonant frequency or a reduced resonator size results in, if the design frequency is to be maintained [34-36]. For the *n*th iteration, the Minkowski-like fractal structures described in Figures-2 have been found to have the perimeters given by:

$$P_n = \left(1 + 2\frac{w_2}{L_o}\right) P_{n-1} \quad (4)$$

where P_n is the perimeter of the nth iteration pre-fractal structure, w_2 and L_o are as shown in Figure-2. Equation (3) and Figure-2 imply that at particular iteration level, a wide variety of structures with different perimeters can be obtained by varying w_1, w_2, or both. It is expected then; further miniaturization can be realized when applying fractal geometries with higher iterations to the conventional SIR ring resonator. The increase in length decreases the required volume occupied for the pre-fractal bandpass filter at resonance. The ability of the resulting structure to extend its perimeter in the successive iterations was found very triggering for considering its size reduction aptitude as a microstrip BPFs.

4. DESIGN AND PERFORMANCE EVALUATION OF THE PROPOSED BPFS

The primary purpose of this paper is to design new BPFs that are characterized by a compact size, a better selectivity, and multiband responses. The design methodology suggested to design these filters is to apply both the SIR approach together with the fractal geometry on the conventional dual-mode square ring resonator BPF as described in Figures 1 and 2. The resulting resonator structure is demonstrated in Figure-3. The steps of the evolution of the new dual-mode resonators result from the application of the SIR technique together with the Minkowski fractal geometry of the 1st and 2nd iterations. In the following sections, the designs of three BPFs based on the structures corresponding to Figures 3(b) to 3(d) will be presented, and their performance will be evaluated in details.

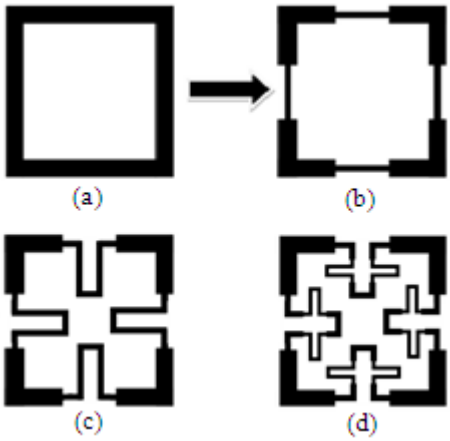

Figure-3. The evolution of the dual-mode resonator; (a) the classical square loop resonator [3], (b) Stepped-impedance square loop resonator [41], (c) and (d) the proposed SIR fractal based BPFs.

4.1 Design of SIR based BPF with zero iteration fractal geometry

The first designed BPF uses SIR technique together with the zero iteration Minkowski fractal geometry as implied from Figure-3(a). The modeled filter structure is shown in Figure-4. According to the design methodology adopted in the present work, this filter can be considered as a Dual-mode SIR based BPF with Zero Iteration Fractal Geometry. The evaluation of the resulting filter responses has been performed using a substrate with a relative dielectric constant (εr) of 10.8 and a thickness (h) of 1.27 mm. Table-1 summarizes of the dimensions of the SIR BPF with the zero iteration fractal Geometry. According to the resonance response, the filter resonator size has been considered in terms of the guided wavelength calculated at the resonant band. For the present case, the filter resonator dimensions are of about 0.3 $\lambda_g \times$ 0.3 λ_g. The corresponding size reduction of the filter is about 40% as compared with the dual-mode square ring resonator BPF.

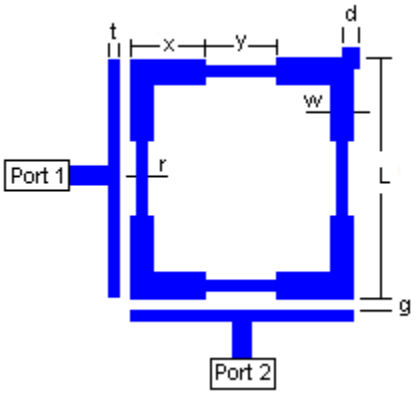

Figure-4. The configuration of the dual-mode SIR BPF with zero fractal iteration.

The simulation results of the input reflection coefficient (S11) and the transmission (S21) responses are demonstrated in Figure-5. It is evident from the results that the resulting BPF possesses a quasi-elliptic transmission response with two transmission zeros.

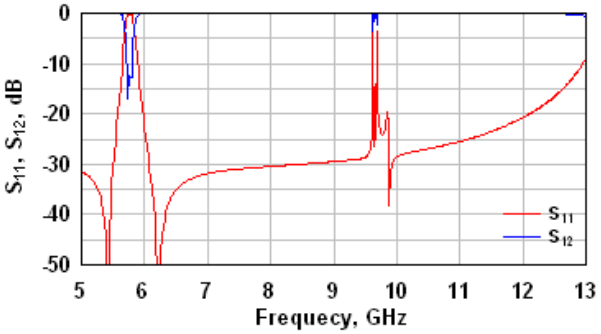

Figure-5. The transmission and input reflection coefficient responses of the bandpass filter with the structure depicted in Figure-4.

The two transmission zeros are asymmetrically situated around design frequency near passband edges. The center of the resonant band is located at 5.8 GHz, and the two transmission poles take place at 5.75 and 5.81 GHz respectively. There is an accepted coupling with S11 and S12 magnitudes of about 22.578 and 0.134 dB respectively. The corresponding bandwidth is found to be about 150 MHz. The bandwidth makes the proposed filter suitable for the WLAN applications.

Table-1. Summary of the dimensions, in mm, of the SIR BPF with the zero iteration fractal Geometry.

Parameters	Values	Parameters	Values
L	5.9	w	0.6
y	1.9	x	2.0
g	0.2	d	0.5
t	0.3	r	0.2
h	1.27		

Examining the results of Figure-5, it is clear that the proposed filter response does not support the second harmonic frequency ($2f$) around 11.6 GHz that typically accompany the performance of the BPFs. Furthermore, the existence of the spurious response at about 9.7 GHz has a little effect on the resulting filter performance. A parametric study is conducted to explore the effect of the perturbation parameter d on the filter performance. Figures 6 and 7 demonstrate the effects of varying d on the input reflection coefficient and the transmission responses respectively. The parameter d has been changed in irregular steps, and the values are chosen according to the apparent change in the resulting filter response. It is apparent that the suggested BPF has a compact size when comparing its dimensions with the guided wavelength at

the design frequency,λ_{g0}. The guided wavelength has been determined at the design frequency (f) by [3]:

$$\lambda_{g0} = \frac{c}{f\sqrt{\varepsilon_e}} \quad (5)$$

$$\varepsilon_e \approx \frac{\varepsilon_r + 1}{2} \quad (6)$$

where c and ε_e represent light speed and effective dielectric constant respectively. However, most of the commercially available EM simulators provide a direct calculation of the guided wavelength at a particular frequency and given substrate parameters. For the existing design, the guided wavelength is calculated to be about 22.294 mm at the design frequency.

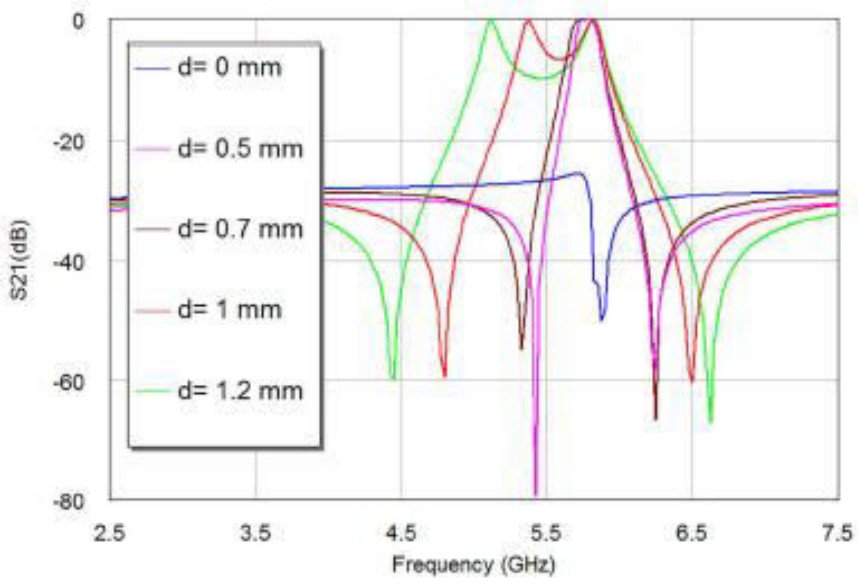

Figure-6. S21 responses of the proposed bandpass filter with d as a parameter.

It is interesting to get more insight of the previous results of the proposed filter in terms of its current distributions. The simulated current distributions on the surface of the filter at the design frequency, 5.8 GHz, are demonstrated Figure-8 for the two cases of the filter structure; with and without perturbation element. The red color represents the high coupling whereas the lowest coupling is indicated by the blue color. Also, the current distribution over all the filter structure has a symmetrical pattern.

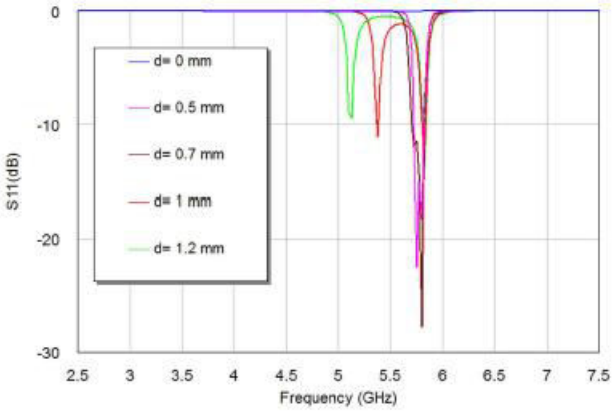

Figure-7. S11 responses of the proposed bandpass filter with d as a parameter.

Table-2. The electrical parameters of the proposed filter concerning d magnitudes (mm).

Parameters	**d = 0**	**d = 0.5**	**d = 0.7**	**d = 1**	**d = 12**
Best S11 in Passband Region (dB)	-----	22.578	27.79	11.07	9.5
Insertion Loss (dB)	-----	0.134	0.24	6.364	9.618
Center Frequency (GHz)	-----	5.8	5.83	5.6	5.474
Bandwidth (MHz)	-----	150	154	546	805
Left and Right Transmission Zeros (dB)	-----	79.35, 57.98	54.86, 66.57	59.48, 60.32	59.92, 67.11
Even and Odd Mode Resonances (GHz)	-----	5.7,5.85	5.66, 5.85	5.326, 5.872	5.067,5.872

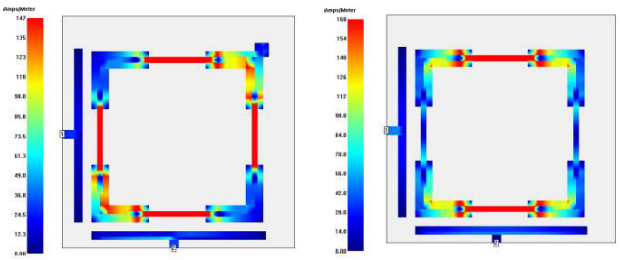

Figure-8. Current intensity distribution of the modeled filter at 5.8 GHz; (a) with perturbation element, and (b) without perturbation element.

To validate the proposed design, a prototype of the filter structure shown in Figure-4 has been fabricated. Figure-9 displays a photo of the fabricated bandpass filter prototype. Figures 10 and 11 demonstrate the measured and calculated S12 and S11 of the fabricated and modeled filters respectively. The measured S11 is about 16.63 dB, and the smallest amount of S12 of the filter is better than 1 dB. The realized bandwidth in the measurement is of about 200 MHz. Table-3 summarizes the measured and simulated values of the proposed filter parameters. There are slight tolerances among the calculated and the measured values; especially for S11, S12 and the realized bandwidth magnitudes. These minor differences are primarily due to conductor loss, port impedance mismatches, and the fabrication tolerances.

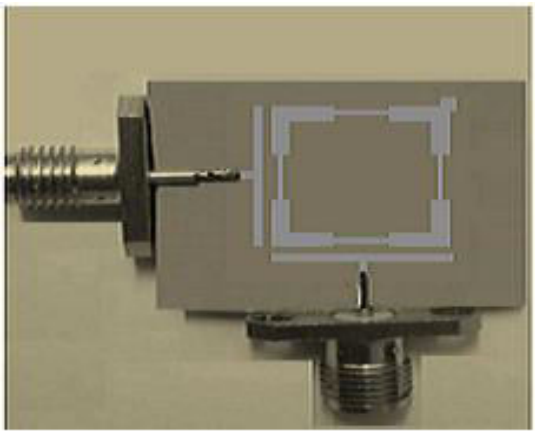

Figure-9. The fabricated bandpass filter prototype.

One of the principal causes of the inaccuracy is the gap width which is considered as a capacitive coupling; any slight difference will affect the resulting filter performance considerably. The effect of the gap width can be with little influence when using a substrate with a low dielectric constant. However, in the suggested design, a suitable substrate material with an appropriate dielectric constant and conductor thickness has been used to improve the filter performance and meet design objectives in that the resulting filter has to be compact and has acceptable characteristics in the passband region.

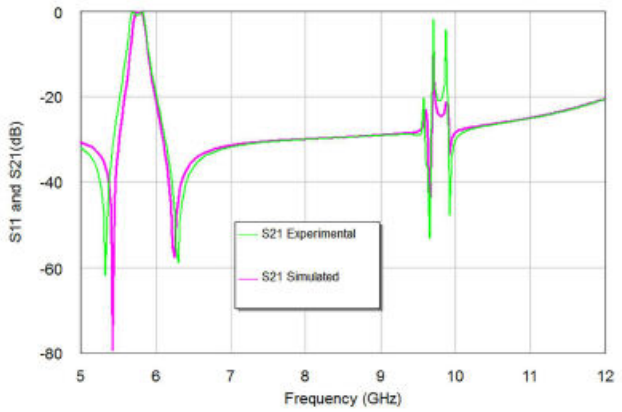

Figure-10. Simulated and experimental S21 responses.

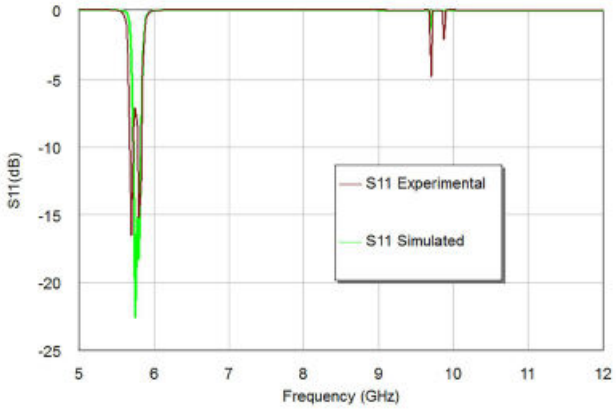

Figure-11. Simulated and experimental S11 responses.

In addition to design simplicity, the measured results of this filter have almost better performance in terms of insertion loss, return loss and bandwidth than those reported in [41–42] under similar center frequency as it can be observed from Table-4. Also, the presented filter design of this study has a small surface area of 0.81cm^2, which is appropriate to be integrated within many wireless systems or communication devices. Regardless of design frequency and electrical filter specifications, the size of this filter is smaller than all designed filters reported in [40–43].

Table-3. Summary of the simulation and measured results for the proposed filter.

Filter Parameters	Sim.	Meas.
Center Frequency (GHz)	5.8	5.8
Insertion Loss (dB) at t he Center Frequency	0.134	0.95
Best Return Loss (dB) in Passband, S11	22.578	16.63
Bandwidth (MHz)	150	200

Table-4. Experimental results of the proposed filter versus those reported in [42] and [43] at 5.8 GHz.

Filter Parameters	This Work	BPF in [42]	BPF in [43]
Insertion Loss (dB), S21	0.95	3.2361	1.821
Best Return Loss (dB) in Passband, S11	16.63	14.502	18
Bandwidth (MHz)	200	750	255
Design Complexity	The simplest	More Complicated	The Most Complicated

4.2 Design of SIR based BPF with first iteration fractal geometry

According to the design methodology adopted in the present work, this filter can be considered as a Dual-mode SIR based BPF with the 1st iteration Minkowski fractal Geometry. The filter structure will be corresponding to that shown in Figure-3(c). This filter has been modeled on the same substrate used in the design of the filter depicted in section 4.1. The layout of modeled filter is shown in Figure-12. Table-5 summarizes the detailed dimensions of the modeled filter.

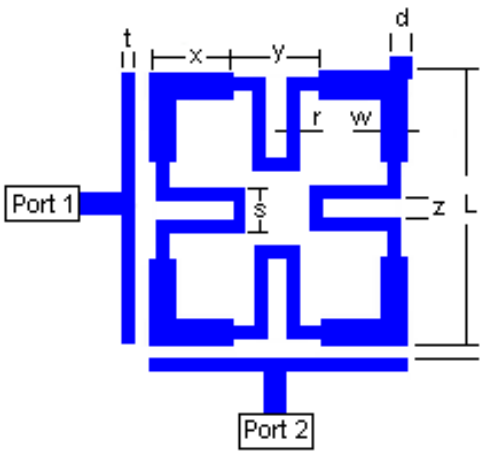

Figure-12. The configuration of the dual-mode SIR BPF with the 1st iteration Minkowski fractal geometry.

The filter size has been maintained unchanged as that for the filter depicted in Figure-4. The simulated S11 and S12 responses of the modeled BPF structure are depicted in Figure-15. It is clear that the filter offers three distinct resonant bands centered at 4.25 GHz, 9.05 GHz, and 12.05 GHz. According to the new resonance response, the filter size has been considered in terms of the guided wavelength calculated at the lower resonant band. For the present case, the filter dimensions are 0.22 $\lambda_g \times$ 0.22 λ_g. The corresponding size reduction of the filter is about 56% in comparison with the dual-mode square ring resonator BPF. The modeled bandpass filter structure can be dimensionally scaled up or down to make applicable to resonate at a specified frequency.

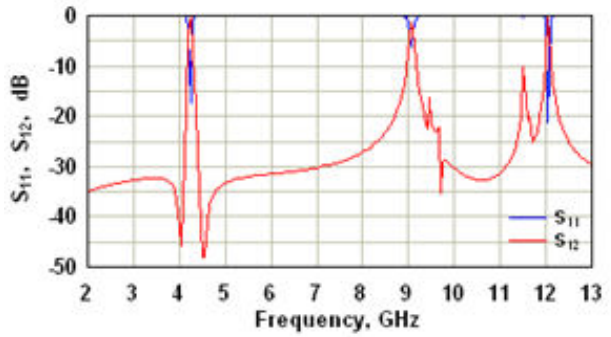

Figure-13. The simulated S11 and S12 responses of the BPF with the structure depicted in Figure-12.

Table-5. Summary of the dimensions of the SIR BPF with the 1st iteration fractal geometry.

Parameters	Values	Parameters	Values
L	5.9	*w*	0.6
y	1.9	*x*	2.0
g	0.2	*d*	0.5
t	0.3	*r*	0.2
h	1.27	*s*	0.69
z	0.5		

The simulated current densities on the surface of the SIR BPF with the 1st iteration fractal Geometry are shown, at different frequencies, in Figure-14.

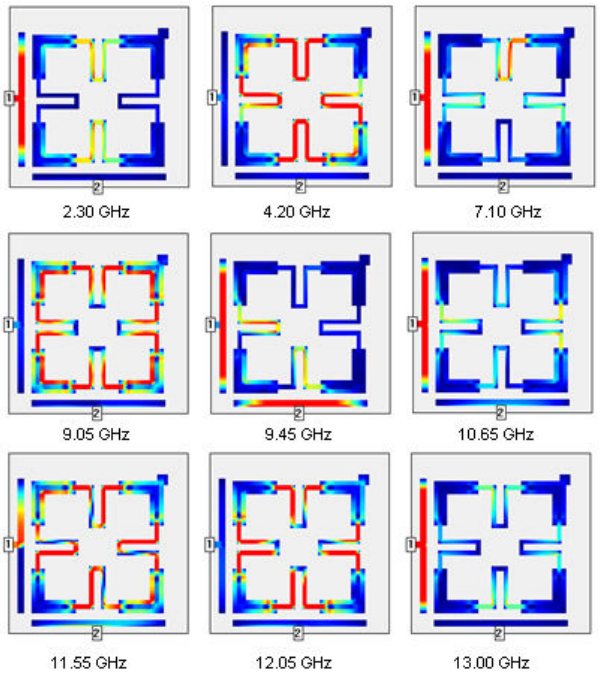

Figure-14. Current intensity distribution of the SIR BPF with the 1st iteration fractal geometry at different frequencies.

4.3 Design of SIR based BPF with second iteration fractal geometry

According to the design methodology adopted in the present work, this filter can be considered as a dual-mode SIR based BPF with the 2nd iteration Minkowski fractal Geometry. The filter structure will be corresponding to that shown in Figure-3(d). The SIR approach has been applied twice to this filter. For this, there are three different transmission line sections; each with its particular width labeled as *w*, *r*, and *v* as shown in Figure-15. This filter has been modeled on the same substrate used in the design of the filters depicted in sections 4.1 and 4.2. The layout of modeled filter is shown in Figure-14. Table-6 summarizes the detailed dimensions of the filter.

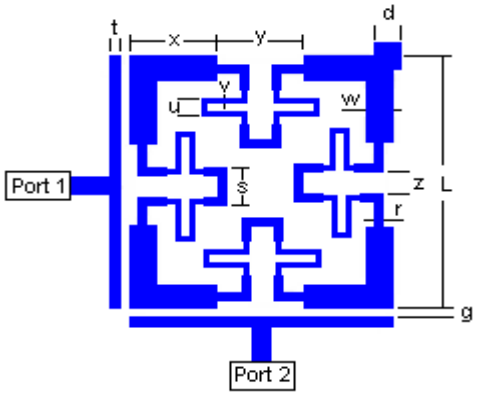

Figure-15. The layout of the dual-mode SIR BPF with the 2nd iteration Minkowski fractal geometry.

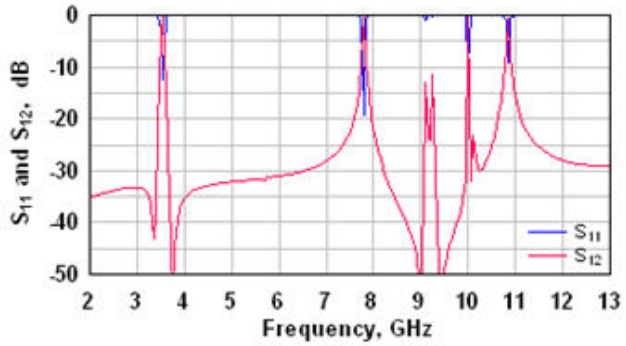

Figure-16. The simulated S11 and S12 responses of the BPF with the structure depicted in Figure-15.

As in section 4.2, the modeled filter size has been kept unchanged at a resonator side length of 5.9 mm. The simulated S11 and S12 responses of the modeled BPF structure are depicted in Figure 16. The results reveal that the filter offers four distinct resonant bands centered at 3.55 GHz, 7.88 GHz, 10.00 GHz, and 10.80 GHz. According to the new resonance response, the filter size has been considered in terms of the guided wavelength calculated at the lower resonant band. For the present case, the filter dimensions are 0.186 $\lambda_g \times$ 0.186 λ_g. The corresponding size reduction of the filter is about 63% in comparison with the dual-mode square ring resonator BPF. Again, the modeled filter structure can be dimensionally scaled up or down to make it applicable to resonate at the specified design frequency. The results of Figure 16 are better understood with the aid of current distribution in Figure-17.

Table-6. Summary of the dimensions of the SIR BPF with the 2nd iteration fractal geometry.

Parameters	Values	Parameters	Values
L	5.9	*w*	0.6
y	1.9	*x*	2.0
g	0.2	*d*	0.5
t	0.3	*r*	0.2
h	1.27	*s*	0.69
z	0.5	*u*	0.42
v	0.2		

The transmission and input reflection coefficient responses of the SIR BPFs with different fractal iteration levels are summarized in Figure-18. Inspection of the results of the results of Figure 18, an interesting finding can be extracted. It is easy to observe that any of the modeled filters offer a number of resonances that progressively increased with the fractal iteration level, plus one spurious resonant band. The filter with zero iteration has one resonant band at 5.8 GHz and one spurious resonant band at 9.62 GHz. Moreover, the filter with 1st iteration fractal geometry possesses two resonant bands centered at 4.25 GHz, 9.05 GHz, and 12.05 GHz and one spurious resonant band at 11.50 GHz. Also, the filter with 2nd iteration fractal geometry possesses three resonant bands centered at 3.55 GHz, 7.88 GHz, 10.00 GHz, and 10.80 GHz, and one spurious resonant band at 9.20 GHz.

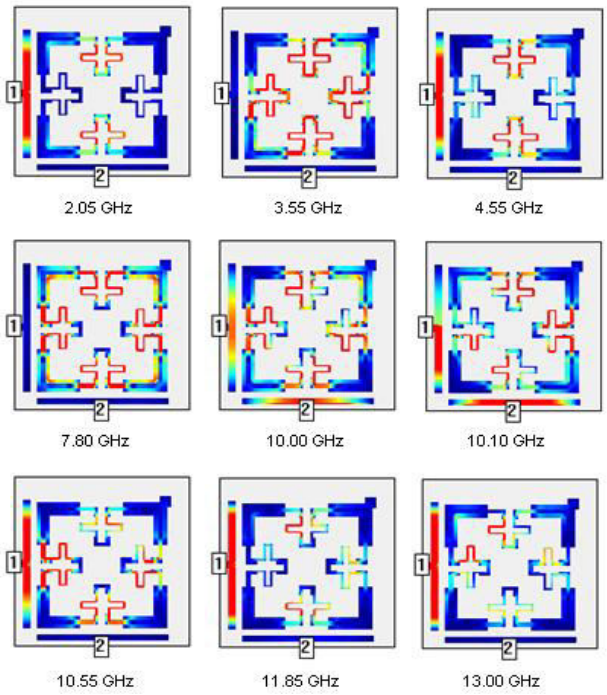

Figure-17. Current intensity distribution of the SIR BPF with the 2nd iteration fractal geometry at different frequencies.

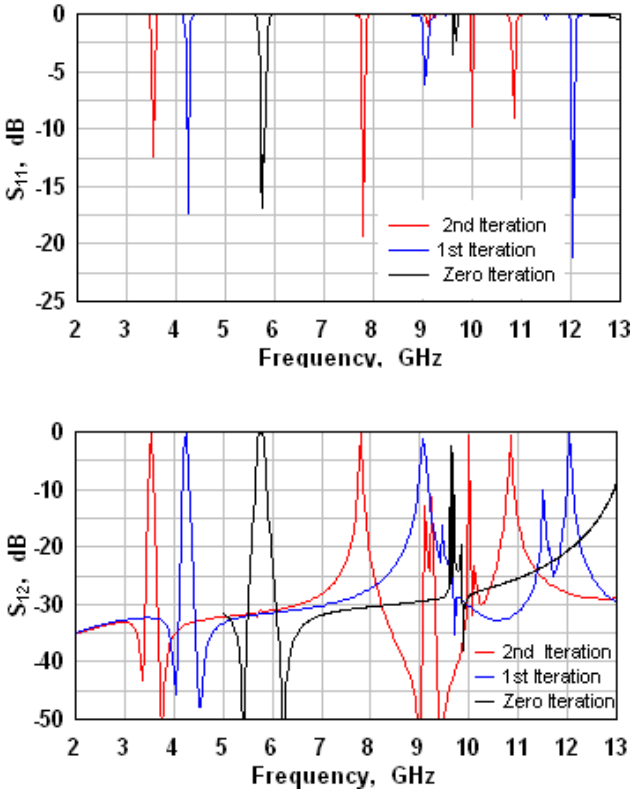

Figure-18. Summary of the transmission and input reflection coefficient responses of the SIR BPFs with different fractal iteration levels.

5. CONCLUSIONS

New compact dual-mode microstrip BPFs with multiband responses are presented in this paper. The design methodology suggested to design these filters is to apply both the SIR approach together with the fractal geometry on the conventional dual-mode square ring resonator BPF. Inspection of the resulting responses of the modeled filters leads to an interesting finding. Besides the achieved size miniaturization, each of the modeled filters offers a number of resonances that progressively increases with the fractal iteration level, plus one spurious resonant band. Experimental results of SIR BPF with zero fractal iteration, designed to operate at 5.8 GHz, agree well with those predicted theoretically. It is planned to fabricate the other two filter based on the 1st and 2nd fractal iteration levels to strengthen the validity of the suggested design methodology.

REFERENCES

[1] P. Jarry and J. Beneat. 2009. Design and Realizations of Miniaturized Fractal Microwave and RF Filters. John Wiley & Sons.

[2] T.C. Edwards and B.S. Michael. 2016. Foundations for Microstrip Circuit Design. John Wiley & Sons.

[3] S. Hong and M. J. Lancaster. 2001. Microstrip Filters for RF/Microwave Applications. John Wiley & Sons, New Jersey.

[4] M. Weng, S. Wu, S. Jhong, Y. Chang, and M. Lee. 2007. A novel compact dual-mode filter using cross-slotted patch resonator for dual-band applications. Proc. of IEEE/MTT-S International Microwave Symposium. pp. 921-924.

[5] V. Crnojević-Bengin, ed. 2015. Advances in Multi-Band Microstrip Filters. Cambridge University Press.

[6] J.K. Ali. 2008. A new miniaturized fractal bandpass filter based on dual-mode microstrip square ring resonator. Proc. of the 5th IEEE International Multi-Conference on Signals, Systems, and Devices, SSD '08; Amman, Jordan. pp. 1-5.

[7] S. Chang, Y. Jeng, and J. Chen. 2004. Dual-band step-impedance bandpass filter for multimode wireless LANs. IET Electronics Letters. 40: 38-39.

[8] S. Sun and L. Zhu. 2005. Compact dual-band microstrip bandpass filter without external feeds. IEEE Microwave and Wireless Components Letters. 15: 644-646.

[9] S. Sun and L. Zhu. 2005. Novel design of dual-band microstrip bandpass filters with good in-between isolation. Proceedings of Asia-Pacific Microwave Conference. pp. 4-7.

[10] M. Mokhtaari, J. Bornemann, and S. Amari. 2006. New reduced-size step-impedance dual-band filters with enhanced bandwidth and stopband performance. Proc. of IEEE MTT-S International Microwave Symposium Digest. pp. 1181–1184.

[11] L. Zhu, H. Bu and K. Wu, and M. S. Leong. 2000. Miniaturized multi-pole broadband microstrip bandpass filter: concept and verification. Proceedings of 30th European Microwave Conference, Paris. pp. 1-4.

[12] P. Mondal and M. Mandal. 2008. Design of dual-band bandpass filters using stub-loaded open loop resonators. IEEE Transactions on Microwave Theory and Techniques. 56: 150-155.

[13] B. Virdee, M. Farhat and K. Ahmed. 2011. Dual-band bandpass filter using open-loop resonators.

Proceedings of Asia-Pacific Microwave Conference. pp. 1054-1057.

[14] E. Babu, M. Ramesh and A. Kalghatgi. 2011. Compact high isolation dual-band bandpass filter. Proc. of 41st European Microwave Conference. pp. 748-750.

[15] W. He, Z. Ma, C. Chen, T. Anada, and Y. Kobayashi. 2008. A novel dual-band bandpass filter using microstrip stub-loaded two-mode resonators with source and load coupling. Proc. of Asia-Pacific Microwave Conference. pp. 1-4.

[16] X. Ma and H. Zheng. 2011. A compact dual-band bandpass filter with adjustable second passband using S-shaped stepped impedance resonator embedded by open stubs. Proc. of Cross Strait Quad-Regional Radio Science and Wireless Technology Conference (CSQRWC). pp. 671-674.

[17] S. Gao, H. Hu and Z. Xiao. 2008. A novel compact dual-band bandpass filter using SIRs with open-stub line. Proc. of Microwave Joint Conference China-Japan. pp. 464-466.

[18] Z. Li and Q. Chu. 2012. Compact dual-band bandpass filter using a novel dual-mode resonator. Proc. of International Conference on Microwave and Millimeter Wave Technology (ICMMT). pp. 1-4.

[19] N. Cohen. 2015. Fractal Antenna and Fractal Resonator Primer, Chapter 8 in J. A. Rock and M. van Frankenhuijsen [Eds.], Fractals and Dynamics in Mathematics, Science, and the Arts: Theory and Applications, Volume 1, World Scientific Publishing.

[20] Y.S. Mezaal, H.T. Eyyuboglu, J.K. Ali. 2013. New dual band dual-mode microstrip patch bandpass filter designs based on Sierpinski fractal geometry. IEEE International Conference on Advanced Computing and Communication Technologies. 3rd, pp. 348-352.

[21] M.H. Weng, L.S. Jang, W.Y. Chen. 2009. A Sierpinski-based resonator applied for low loss and miniaturized bandpass filters. Microwave and Optical Technology Letters. 51: 411-13.

[22] C.S. Ye, Y.K. Su, M.H. Weng, H.W. Wu. 2009. Resonant properties of the Sierpinski-based fractal resonator and its application on low-loss miniaturized dual-mode bandpass filter. Microwave and Optical Technology Letters. 51: 1358-61.

[23] Y.S. Mezaal, H.T. Eyyuboglu, J.K. Ali. 2014. Wide bandpass and narrow bandstop microstrip filters based on Hilbert fractal geometry: design and simulation results. PloS one. 9: 1-12.

[24] J. Chen, Z.B. Weng, Y.C. Jiao, F.S. Zhang. 2007. Lowpass filter design of Hilbert curve ring defected ground structure. Progress In Electromagnetics Research. 70: 269-80.

[25] Y.S. Mezaal, H.T. Eyyuboglu, J.K. Ali. 2013. A novel design of two loosely coupled bandpass filters based on Hilbert-zz resonator with higher harmonic suppression. Proc. IEEE 3rd International Conference on Advanced Computing and Communication Technologies, (ACCT). pp. 343-347.

[26] Y.S. Mezaal, J.K. Ali, H.T. Eyyuboglu. 2015. Miniaturised microstrip bandpass filters based on Moore fractal geometry. International Journal of Electronics. 102: 1306-19.

[27] T.P. Li, G.M. Wang, K. Lu, H.X. Xu, Z.H. Liao, B. Zong. 2012. Novel bandpass filter based on CSRR using Koch fractal curve. Progress In Electromagnetics Research Letters. 28: 121-28.

[28] J.K. Ali, Y.S. Miz'el. 2009. A new miniature Peano fractal-based bandpass filter design with 2nd harmonic suppression. Proc. of the 3rd IEEE International Symposium on Microwave, Antenna, Propagation and EMC Technologies for Wireless Communications. pp. 1019-1022.

[29] J.K. Ali, H. Alsaedi, M.F. Hasan, H.A. Hammas. 2012. A Peano fractal-based dual-mode microstrip bandpass filters for wireless communication systems. Proc. of Progress in Electromagnetics Research Symposium. pp. 888-892.

[30] Y.S. Mezaal, H.T. Eyyuboglu, J.K. Ali. 2013. A new design of dual band microstrip bandpass filter based on Peano fractal geometry: Design and simulation results. Proc. of the 13th IEEE Mediterranean Microwave Symposium, MMS'2013. pp. 1-4.

[31] J.K. Ali, N.N. Hussain. 2011. An extra reduced size dual-mode bandpass filter for wireless communication systems. Proc. of Progress in Electromagnetics Research Symposium. pp. 1467-70.

[32] J.C. Liu, H.H. Liu, K.D. Yeh, C.Y. Liu, B.H. Zeng, C.C. Chen. 2012. Miniaturized dual-mode resonators

with Minkowski-island-based fractal patch for WLAN dual-band systems. Progress in Electromagnetics Research. 26: 229-43.

[33] A. Lalbakhsh, A. Neyestanak, M. Naser-Moghaddasi. 2012. Microstrip hairpin bandpass filter using modified Minkowski fractal-shape for suppression of second harmonic. IEICE Transactions on Electronics. E95C (3): 378-381.

[34] M. Alqaisy, J.K. Ali, C.K. Chakrabarty, G.C. Hock. 2013. Design of a compact dual-mode dual-band microstrip bandpass filter based on semi-fractal CSRR. Progress in Electromagnetics Research Symposium. pp. 699-703.

[35] M. Alqaisy, C. Chakrabraty J.K. Ali, A.R.H. Alhawari. 2015. A miniature fractal-based dual-mode dual-band microstrip bandpass filter design. International Journal of Microwave and Wireless Technologies. 7: 127-133.

[36] J.K. Ali, N.N. Hussain, A.J. Salim, H. Alsaedi. 2012. A new tunable dual-mode bandpass filter design based on fractally slotted microstrip patch resonator. Progress in Electromagnetics Research Symposium Proceedings. pp. 1225-1228.

[37] J.K. Ali and H.T. Ziboon. 2016. Design of compact bandpass filters based on fractal defected ground structure (DGS) resonators. Indian Journal of Science and Technology. 9: 1-9.

[38] J.K. Ali and H. Alsaedi. 2012. Second harmonic reduction of miniaturized dual-mode microstrip bandpass filters using fractal shaped open stub resonators. Proc. Progress in Electromagnetics Research Symposium. pp. 1266-1269.

[39] H.T. Ziboon and J.K. Ali. 2017. Compact dual-band bandpass filter based on fractal stub-loaded resonator. Proc. Progress in Electromagnetics Research Symposium.

[40] Y.S. Mezaal, H.T. Eyyuboglu, J.K. Ali. 2014. New microstrip bandpass filter designs based on stepped impedance Hilbert fractal resonators. IETE Journal of Research. 60: 257-64.

[41] Y.S. Mezaal, J.K. Ali. 2016. Investigation of dual-mode microstrip bandpass filter based on sir technique. PLoS ONE. 11: 1-14.

[42] M.A. Othman, M. Sinnappa, M.N. Hussain, M. Z. A. Abd-Aziz, M.M. Ismail. 2013. Development of 5.8 GHz microstrip parallel coupled line bandpass filter for wireless communication system. Intern. Journal of Engineering and Technology. 5: 3227-3235.

[43] C. Lugo, D. Thompson, J. Papapolymerou. 2003. Reconfigurable bandpass filter with variable bandwidth at 5.8 GHz using a capacitive gap variation technique. 33rd European Microwave Conference. pp. 923-926.